

# Tether Gravity Gradiometer for Planetary Missions

Principal Investigator: Robert B. Sheldon

Email: [rbs@rbsp.info](mailto:rbs@rbsp.info)

## Table of Contents

I. Scientific/Technical/Management.....	1
A. Executive Summary.....	1
B. Need for planetary gradiometry.....	2
C. Development of a tether gradiometer.....	3
D. Development of a Cubesat gradiometer.....	6
E. The operations of the Cubesat.....	7
Management.....	8
References.....	9
II. Current and Pending Support.....	9
Dr. Robert Sheldon.....	9
Dr. Bogdan Udrea.....	9
Dr. Hien Vo.....	10
Dr. Eric Todd Bradley.....	10
Mr. Alvin Eric Cantrell.....	11
III. Statements of Commitment.....	11
IV. Budget Justification: Narrative and Details.....	16
Grassmere Dynamics, LLC: Robert Sheldon.....	16
Embry-Riddle University: Bogdan Udrea.....	16
University of Central Florida: Eric Todd Bradley.....	16
University of Turabo, Puerto Rico: Hien Vo.....	17
V. Facilities and Equipment.....	23
VI. Special Notifications and/or Certifications.....	24
VII. Table of Personnel and Work Effort.....	24
Dr. Robert Sheldon.....	24
Dr. Eric Todd Bradley.....	24
Dr. Bogdan Udrea (ERAU) and Dr. Hien Vo (SUAGM).....	24
Mr. Alvin Eric Cantrell.....	25
Sr. Electronics Engineer.....	25
VIII. Biographical Sketches.....	26
Dr. Robert B. Sheldon.....	26
Dr. Bogdan Udrea—Co-I.....	28
Dr. Hien Vo—Co-I.....	29
Dr. Eric Todd Bradley —Co-I/Science-PI.....	30
Mr. Alvin Eric Cantrell—Co-I.....	31

# I. Scientific/Technical/Management

## A. Executive Summary

Flybys of planets and moons revealed surprising dynamics occurring below the visible surface: Io's volcanoes are supplied by an underground lava supply; oceans at Europa swirl beneath a thick cap of ice; and Venus' active volcanism lays under an obscuring blanket of clouds. Satellite-borne gravity gradiometers like GRACE and GOCE have proved indispensable in low Earth orbit, characterizing changing ice mass, magma intrusions, or water transport, while GRAIL revolutionized lunar geology models. But for planetary missions, the cost and control of a dual-satellite gradiometer has seemed beyond reach, despite real progress in miniaturizing the sensors.

**This proposal addresses the real need for a New Frontiers gravity gradiometer.**

Long before these accelerometer-based missions, NASA studied a mission to measure the gravity gradient directly by monitoring the tension in a 1km tethered 115kg dumbbell satellite [Colombo, 1979]. It was capable of GRACE-like sensitivity, but it commandeered the entire spacecraft, and gradiometers had not yet proven their worth. Thirty-five years later satellites are small enough that the s/c bus, the instrument, and two 200m tethers can be integrated on a single 6U Cubesat—11x14x37cm and 12kg. **The tether gradiometer not only measures the vertical gradient with 5X more sensitivity, but with a resolution 15X higher due to its smaller mass.**

Since the instrument is the s/c, it is a free flier deployed from a mother s/c, permitting injection into a low altitude orbit with increased S/N and spatial resolution. In atmospheres, drag can be matched between Cubesat and endmass by adjusting the solar-panel angle of incidence, permitting common mode rejection down to the  $<1$  ppm level. Thermal fluctuations caused by orbiting in/out of sunlight are minimized using ultra low expansion glass-fiber tether, with  $\sim 1$  ppm noise signal. Swaying errors are resolved  $<1$  ppm by lighting the fiber with an LED and imaging the endmass position to  $<0.03^\circ$ . Glass-fiber tethers resist the radiation environment of the Jovian magnetosphere, while the electronics are passively shielded. A low power FPGA compresses the digitized tension before transmission to the mother ship, with minimal telemetry and power. **The venerable tether gradiometer has become a capable, 21<sup>st</sup> century sensor.**

**Objectives:** We will **(1)** integrate a unique, low-noise gravity gradiometer developed at NASA over the past 40 years with a 6U Cubesat along with accompanying radiation hardened computer and electronic hardware; **(2)** adapt existing tethers to fit within the 6U Cubesat to be deployed in orbit, testing and validating the most common failure mode for tethers; **(3)** use the Globalstar satellite network as a mother-ship relay test, simulating actual low-bitrate operation at an extraterrestrial planet; **(4)** utilize a NASA CSLI launch opportunity to deploy in low Earth orbit, using the South Atlantic Anomaly to test radiation resistance, with known Earth calibration targets: Arctic vs Antarctica for Europa; Himalayan/Andes for Moon/Venus; and Ring-of-Fire (Wolf/Sakurajima) vs plume (Kilauea) volcanoes for Io; **(5)** develop a model with Cubesat orbital parameters, instrument performance, and estimated gravity gradients (due to lava tubes, variations in geological features, thermal gradients) to predict S/N for future New Frontiers AOs.

These tasks will “...mature proposed technologies and reduce their technical risk such that the accompanying mission concepts are better prepared for the next two New Frontiers AOs.” Few sensors can deliver global details of the interiors of Europa, Saturn, Io or Venus. Few sensors have been so well studied while waiting for a s/c with Cubesat capabilities. Few sensors have ppb sensitivities. It is a rare synergy that brings these technologies together after 40 years.

**The global mapping of subsurface geology provides a key capability for New Frontiers.**

## B. Need for planetary gradiometry



Figure 1: L: Lava tube from Hawai'i Volcanoes Nat'l Park. R: Modelled Io lava tubes.

Remote sensing of the surface of a planet/moon only provides part of its evolutionary history. Subsurface observations are essential to form a complete picture of the evolutionary processes that have occurred from formation through the current day. At Earth, gravity gradiometers have convincingly demonstrated the importance of mapping the subsurface structures. GRACE observed the subsurface flow of water and magma; GRAIL mapped the structure of the lunar crust and lithosphere. The surfaces of bodies with thick atmospheres, e.g., Saturn or Venus, are not observable by many remote sensing instruments, so without gravity probes to look beneath the surface very little may be determined about the geological processes that have occurred throughout the formation and evolution of the body.

Investigations of the outer solar system by Voyager, Cassini and HST as well as ground-based observations demonstrate that dynamical processes are occurring beneath their atmospheres and surfaces. Volcanism on Io due to tidal flexing of its eccentric orbit around Jupiter cannot be modelled without mapping the spatial distribution of lava channels and the total amount of mass of lava beneath the surface. The water ocean on Europa lies hidden under a thick layer of ice so that the extent and mass of the subsurface ocean is invisible to all remote sensing except gravity gradiometry, yet this ocean may harbor the greatest chance for life outside of Earth. Water geysers on Saturn's moon Enceladus have revealed not just the possibility of liquid water beneath the surface but organic constituents as well. Saturn's moon Titan has a thick

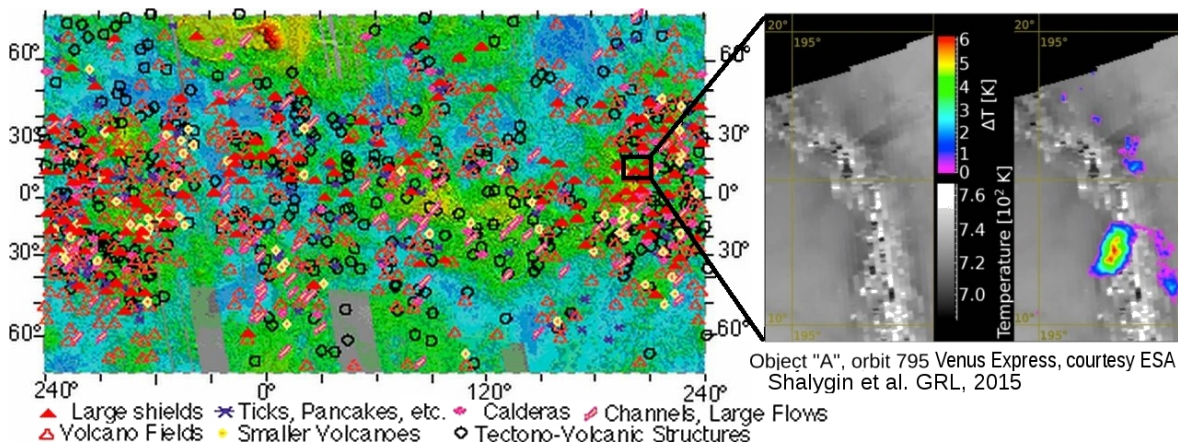


Figure 2: L: Volcanic activity and structures on Venus. R: IR image showing dynamic activity.

nitrogen atmosphere, which Huygens penetrated for a brief 90 minutes to take a snapshot of hidden methane rivers, but a gravity gradiometer could characterize the dynamic processes of the global methane cycle and perhaps even that of water beneath the surface.

*This makes our proposed gravity gradiometer relevant to at least three of the seven mission concepts included in the decadal survey list: Jupiter's moon Io; a Venus In Situ Explorer; and a Saturn probe.* Figure 1 demonstrates the need for subsurface observations of Io where lava flows beneath the surface erupt in a dynamically changing environment. Io's radius of 1,821 km has little surface relief or atmosphere permitting perhaps 10km altitude orbits of 106 minutes at 1.8 km/s. A polar orbiting gravity gradiometer sampling at 2Hz would map spatial variations to ~4km scales and globally on time scales of days, providing global averages of magmatic material. Figure 2 shows the volcanic activity on Venus, where like Io, the gravity gradiometer orbiting ~180km could map magmatic activity to <100km scales on time scales of days. At Saturn, free-flying gravity gradiometers are versatile enough to look for variations within the thick atmosphere,

characterize the gravity instabilities of the ring particles, as well as monitor subsurface activity of moons such as Titan and Enceladus. The left panel of Figure 3, shows variations in Saturn's moon Titan around hydrocarbon lakes made of liquid methane or ethane, which will be constrained by gradiometry. The right panel shows a model of the interior of Enceladus, which may contain a liquid water ocean. Erupting water ice plumes have been observed suggesting a liquid ocean beneath the surface, which a gravity gradiometer could characterize.

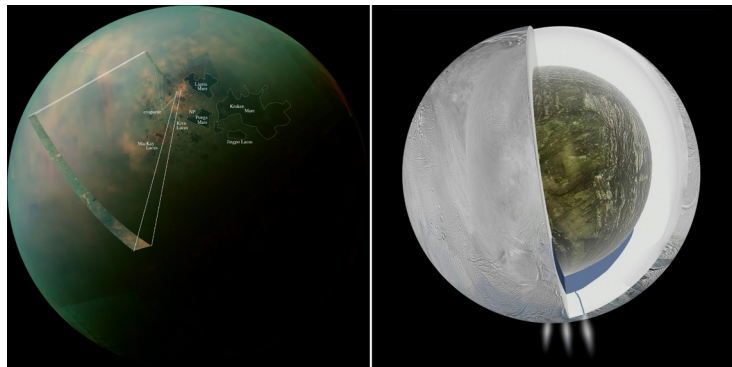


Figure 3: L: Surface composition variation near hydrocarbon lakes of Titan (NASA). R: Model of Enceladus with interior water ocean and plumes.

To achieve these science objectives we will simulate gravity observations with the modelling tool of goal 5, which will be developed by the science PI using Cubesat orbital parameters, instrument performance, and a model of gravity gradients to predict S/N values. **This iterative approach will predict orbital parameters, integration periods, and ultimately the specifics of the science goals for a New Frontiers mission such as the achievable spatial and temporal resolution of subsurface magmatic activity.**

### C. Development of a tether gradiometer

The NASA tether gradiometer is a recent technology development building upon whitepapers commissioned over 35 years ago, which showed that the gravity gradient signal is linearly proportional to the length (L) of the tether and the size of the endmass (M),  $\text{Signal} = 0.75 \cdot LM\Gamma_{zz}$ , where  $\Gamma$  is the gravity gradient tensor. The responsiveness, or natural frequency of the tether, is proportional to  $1/\sqrt{LM}$ , and opposite to sensitivity, causing Bortolami (1995) to optimize the length at 1km with 114kg endmass, which at 230km altitude, achieved GRACE-quality data (Figure 3). **The 1000X reduction of noise of this proposal, increases S/N by 1000X, permits reducing the endmass by 1/40 (3.5kg) and the tether length by 1/5 (200m), for a net gain 5X in sensitivity, 15X in faster response (with less resonance with the signal), higher spatial resolution, and most important of all, integration on a Cubesat spacecraft.**

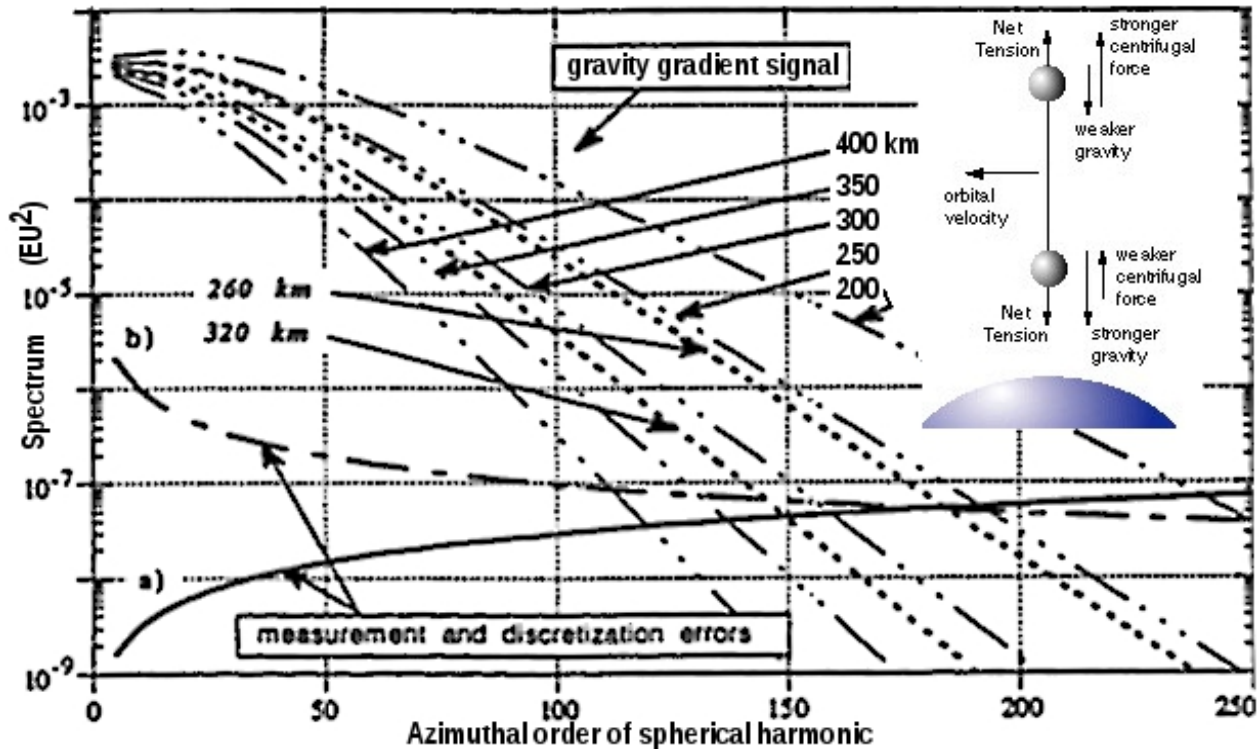


Figure 4: Sensitivity/resolution of tether gradiometry versus altitude. S. Bortolami 1995.

There are three types of noise to consider: atmospheric disturbances, perturbations of the endmasses, and electronic or transducer noise. Atmospheric noise is hardest to remove, because the sensitivity of any gradiometer is improved by lowering the altitude, which is precisely where the atmosphere is most dense. Fortunately Io's atmosphere is tenuous, but remains a concern for Saturn and Venus. We compensate for drag first by flaring the solar panels to roughly match the drag between Cubesat and endmass, and then by monitoring the angle between spherical endmasses so that total tension and trigonometry permit subtraction of the drag forces. Then *ppm* signal can be extracted at ~230km altitude at Earth, or the same low-altitude orbits as GOCE.

The perturbation or swaying of the tether is compensated similarly, resolving the angle between Cubesat and LED-fiber illuminated endmass to within 0.03°, which is achieved in the nadir direction with a 30 MPixel camera and a 180° fisheye lens to capture the limb and endmass in the same frame, while in the zenith direction the star camera achieves 0.01°. According to Bortolami 1995, ~0.03°rms reduces the uncertainty to 0.001EU, or <1 *ppm* EU<sup>2</sup> (where 1 EU=1 ng/m), which gives comparable S/N as the drag noise.

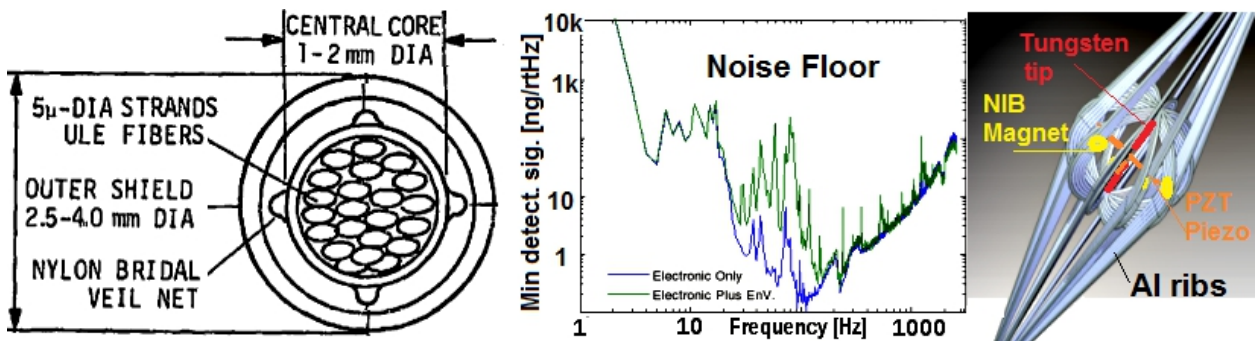
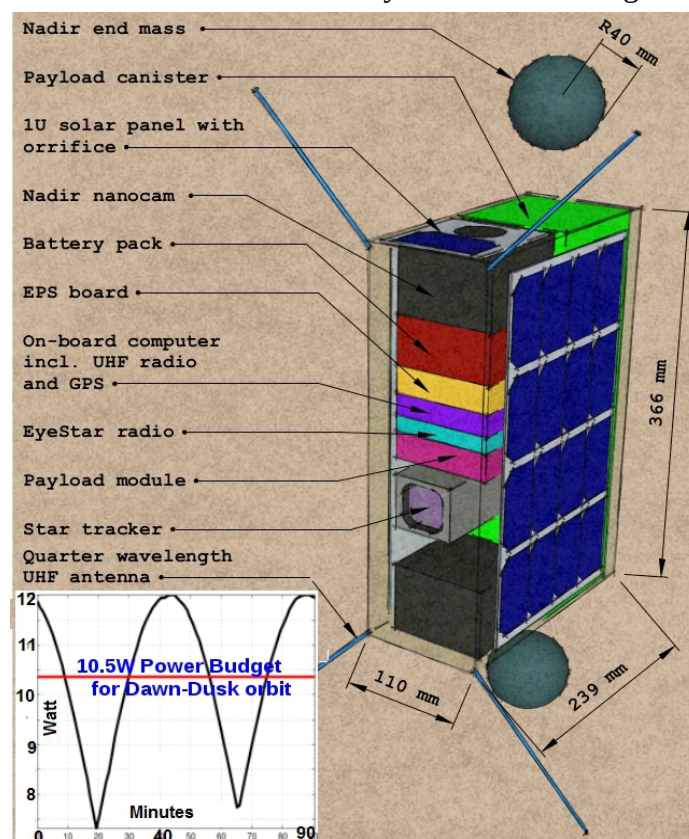


Figure 5: L: Multistrand tether design 1979. M: Noise floor vs Hz, 2014. R: Tension transducer with piezo in center and rib magnets providing positive tension as well as magnetic damping.

Finally, the transducer noise is minimized by using a point-contact piezo force sensor, where the noise is proportional to the area (and volume) of the strained piezo material. **Our novel design (Fig. 4 right panel) converts the tension into a (magnetically buffered/damped)  $\sim 1\text{mm}^2$  point compression of a thin PZT piezo with a noise floor 0.1-0.001X less than commercial tensiometers.** Using low-noise pre-amplifiers with state-of-the-art 24-bit digitizers we can extract  $ppb$  ( $10^{-9}$ ) precision from the tension measurement, sampling at 100Hz and averaging to 10Hz science data, where the natural longitudinal frequency of our endmass is  $\sim 2\text{Hz}$ . At Earth, the orbital speed of 7.7km/s converts this sample rate into  $\sim 770\text{m}$  spacing along the s/c track having a spherical harmonic  $k > 2000$ , which is far too fine for Earth, since the horizontal resolution of  $\Gamma_{zz}$  is approximately equal to orbital altitude, but this sample rate is relevant to airless moons and tenuous atmospheres where orbital altitude can be lowered to the limits of surface topography.

Ground testing of the sensor (“Point Mechanic Piezoelectric Sensor System,” Inventors: Richeson et al., Docket No. MFS 32945, Fig 4. middle panel) performed by Ducommun Miltec 12/2014, under NASA Contract No. NNM14AD98P demonstrated a 5.12 ksamples/s with a noise of 0.4nV/rtHz at 1kHz. Converting this into a force, the minimum detectable signal (the noise floor) was found to be 1.5 nN/rtHz at 113Hz for a 1.5kg mass of 15N, achieving  $\sim 15\text{nN}/15\text{N}$  or  $ppb$  ( $10^{-9}$ ) sensitivity. When compared to commercial accelerometers—Omega ACC103, PCB Piezo-tronics 393B31, and Measurement Specialties Model 4807A—this device is 1000, 10, and 2000 times more sensitive respectively because of its novel point contact design.

The [Colombo 1979] design selected Ultra-Low-Expansion glass for its tether, left panel Figure 4, in order to minimize thermal fluctuations caused by changing solar illumination from the unavoidable 90-minute orbital period. With a 0.03  $ppm$  thermal coefficient of expansion, the additional noise introduced by thermal stretching can be reduced to the same magnitude as the



angular perturbations. The same LED that lights the glass tether to illuminate the endmass for the precision angular measurement can be pulsed/comb modulated to acquire time-domain reflectometry of the  $\sim \text{mm}$  distances using electronic shuttering of the camera for timing.

Since glass tethers suffer from limited radii of curvature, the multistrand design of Figure 4 maximizes flexibility without sacrificing overall strength. For typical tensile strength values of  $>3\text{GPa}$ , a  $5\mu$  diameter fiber has a strength of 60 mN. Then a 35N total strength (the force at 1g on a 3.5kg, 7cm diameter tungsten ball) is achieved with bundle of 500 fibers, with an inner core diameter of some 0.12mm. A Teflon outer shield over bridal net provides thermal insulation and low-friction assistance to the deployer. While specifics of radiation hardness depend on the exact chemical composition of the glass, typical

Figure 6: 6U Cubesat Schematic

ULE-glass has only 5-10% loss in tensile strength after exposures up to  $10^{20}$  NVT neutrons or gamma radiation up to  $10^5$  J/g, but no degradation from UV. *With margin, this makes it ideal for the high radiation environment of the Io torus.* Both the tether and the deployer will be provided by Tethers Unlimited, a leading provider of space tethers and deployers with multiple s/c successes to their credit.

With the sensitivity established in ground testing, the lowest TRL and highest risk component of the instrument remains the tether and its space deployment. **Therefore it is essential that instrument development include a Cubesat engineering proof-of-concept launch to validate its ground-breaking capabilities for a New Frontiers mission.**

## D. Development of a Cubesat gradiometer

**Dr. Bogdan Udrea has obtained a Cubesat Launch Initiative slot for the launch of a 6U Cubesat in 2016.** It has dimensions of (113×239×366) mm and a mass of 12 kg and thus satisfies the requirements of the Planetary Systems Canisterized Satellite Dispenser (CSD). During nominal operations the nanosatellite is gravity stabilized by the means of two end masses that are symmetrically deployed at the end of 200m ULE glass tethers. The passive gravity gradient stabilization is augmented by a set of three mutually orthogonal magnetorquers which are used to detumble the nanosatellite after deployment, orient it after detumble, and damp undesired oscillations after endmass deployment. The magnetorquers are embedded in solar panels and each produces a dipole moment of  $0.188 \text{ A m}^2$ . A 3-axis magnetometer and a star tracker are used as primary attitude determination sensors. The magnetometer is mainly used during the detumbling phase and the star tracker is used in the nominal, or science, phase of the mission. The solar panels are used as coarse Sun sensors that operate together with the magnetorquers to determine the attitude of the nanosatellite in case of star tracker malfunction. The magnetometer is embedded in a Sparton inertial measurement unit (IMU), the GEDC-6EP, and has range of  $\pm 1.2$  Gauss. The star tracker, from Blue Canyon Tech, is accurate to 6 arcsec about the boresight and 40 arcsec about the roll axis.

The orbital position, velocity, and time are obtained from a NovaTel OEM615 board that operates with the L1/L2/L2C GPS and L2/L2 GLONASS systems. The electrical power subsystem (EPS) consists of components from ClydeSpace, specifically two 6U, one 3U, and one 1U solar panels, the 3G Flex EPS power regulation and distribution motherboard and, a 30 Whr battery pack. All solar panels are body fixed with flare hinge.

The communications subsystem consists of two radios:

GomSpace UHF transceiver; and Near Space Launch EyeStar S2 GlobalStar transmitter. The

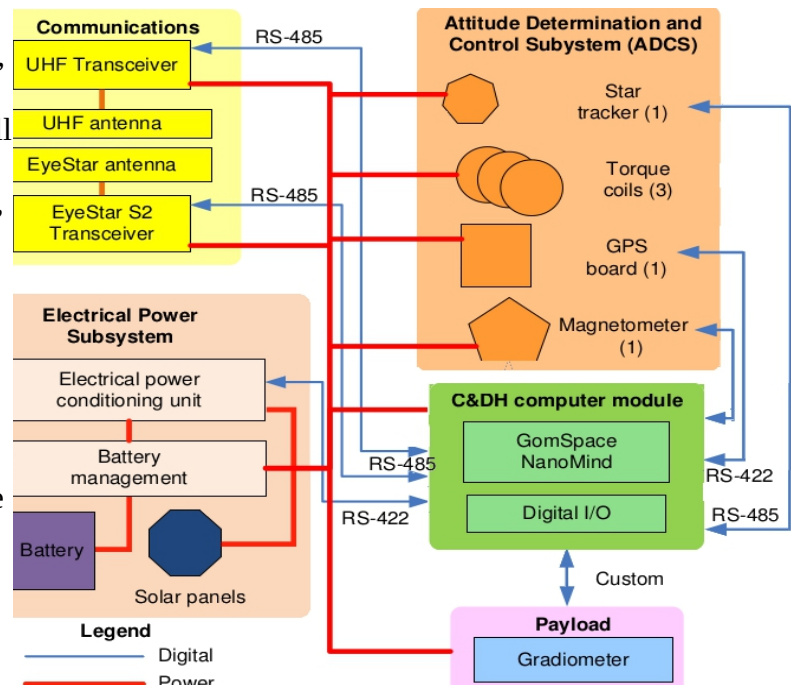


Figure 7: Functional block diagram

UHF transceiver is used for both the uplink of commands and downlink of housekeeping and science data and beaoning. The EyeStar transmitter is used as emulator for the communication link with the mothership for deep space missions of the Cubesat. The UHF transceiver is connected to a quadrupole 1/4 wavelength antenna and the EyeStar is connected to its patch antenna. The on-board computer consists of a GomSpace Nanomind A712D on-board computer (OBC). The GomSpace Nanodock motherboard carries the OBC, the GPS board, and the UHF transceiver, which interfaces the OBC with the sensors and actuators of the attitude determination and control system (ADCS), the EPS motherboard, and the payload electronics module.

The structure of the nanosatellite will be hogged out of large piece of Al 6061 alloy in the shape of a two 3U (113×120×366)mm boxes. One box contains the nanosatellite, payload electronic modules and the star tracker. Its walls will be reinforced with polyethylene/Pb to shield the electronics from energetic particles. The second box will contain the restraining and deployment mechanism for the end masses, tethers and the gradiometer transducer. The only deployables are the end masses and their tethers and the UHF antennas. A preliminary design of

Component	Power (W)	Power Nom.	Power idle	Units	Duty cycle	Orbit avg
1 Magnetorquers	0.50	0.000	0.000	3	5%	0.08
2 3G Flex EPS Motherboard	1.60	0.160	0.160	1	66%	1.11
3 Nanomind A712D On-board computer	0.23	0.000	0.000	1	100%	0.23
4 Nanocom AX100 UHF transceiver	2.64	0.182	0.182	1	10%	0.43
5 Nanomind ADCS interface	0.13	0.000	0.000	1	100%	0.13
6 GPS board	1.00	0.000	0.000	1	100%	1.00
7 EyeStar S2 radio	2.50	0.002	0.002	1	2%	0.05
8 Star tracker	0.75	0.500	0.500	1	100%	0.75
9 Nanocam	0.36	0.000	0.000	2	95%	0.69
10 IMU	0.32	0.012	0.012	1	10%	0.04
11 Payload	1.00	0.000	0.000	1	95%	0.95
<b>Total (W)</b>						<b>5.46</b>
Orbit avg power sun-synch	7.30			Cont. (%)		25%
Orbit avg power sun-synch dawn-dusk	10.30			Cont. (%)		47%
<b>Comments</b>						
1.Magnetorquers embedded in solar panels - they are all the same size						
2.Power draw based on an assumed efficiency of 80% of 20W EPS board						
3.GomSpace - based on 3.3Vx70mA supplied voltages and current						
4.GomSpace - 3.3Vx800mA for transmit (55mA for receive)						
5.GomSpace - 3.3Vx40mA supplied voltages and current						
5.Novatel OEM615						
7.NearSpaceLaunch simplex Globalstar radio						
3.BCT star tracker - quote is one year old						
7.Gomspace - Nanocam based on 3.3Vx110mA max. current						
10.Sparton IMU - GEDC-6EP						
11.Preliminary data from Rob Sheldon						

Figure 8: Operating power budget

the satellite is shown in Figure 5 together with a functional diagram in Figure 6 that has been used to account the data and power interfaces. Analysis of the power generation in a 300 km circular Sun synchronous orbit is shown in Figure 5 inset. The orbit average power (OAP) in a dawn-dusk Sun synchronous orbit is 10.3W. The power budget during the science phase of the mission, shown in Figure 7, shows that the nanosatellite is power positive. The OAP margin is 25% for the generic Sun synchronous orbit and 47% for the dawn-dusk orbit shown (inset Figure 6).

The components of the nanosatellite bus have technology readiness levels between 6 and 9. **The payload has a TRL 4 which this proposal will raise to TRL 6.**

## E. The operations of the Cubesat

**The nanosatellite will be operated as a discrete state machine with a certain number of mission modes or super-states, which simplifies operations and prevents non-recoverable states.** The state of each of subsystem is a sub-state of a mission mode and the transition between states are triggered on conditions of pertinent subsystems. The modes that have been identified at this stage of mission design are itemized below together with a brief description.

\* *Storage* – the nanosat is in its CSD with all power off – transition to *Ejected* is performed on throwing two pressure switches at the release of the door switch.



## References

- A.E. Cantrell, J.J. Richeson, M.D. Sloan, K.S. Srinivasan (2015) “Piezoelectric Gravity Gradient and Multiple Purpose Sensor Detection System.”, *MSFC Patent Application MFS-32945-1*, Serial No. Pending.
- Ducommun Miltec,(2014) “Novel NASA vibration sensor”, *NASA Contract #NNM14AD98P*, Dec 19, 2014.
- Giuseppe Colombo, Arnold, D. A., Binsack, J. H., Gay, R. H., Grossi, M. D., Lautman, D. A., and Orringer, O. (1976) “Dumbbell-gravity gradient sensor: A new application of orbiting long tethers”. *Reports in Geoastronomy 2*, Smithsonian Astrophysical Observatory.
- Giuseppe Colombo, (1979) “System Noise Analysis of the Dumbbell Tethered Satellite for Gravity-Gradient Measurements”, *Tech Report #NASA-CR-162333*.
- Joseph A. Carroll (1985) “Guidebook for Analysis of Tether Applications”, Martin Marietta, *Tech Report #RH4-394049*, NASA/MSFC contract #NAS8-35499 “Phase II Study of Selected Tether Applications in Space”.
- S. B. Bortolami, F. Angrilli, C. Jekeli, M. D. Grossi, (1995) “Analysis of a Dumbell Sensor for Space Gradiometry”, in *Proc. Of Fourth International Conference on Tethers in Space*.

## II. Current and Pending Support

### Dr. Robert Sheldon

#### Current

Project/Proposal Title: Consulting  
Source of Support: Torch Technologies  
Total Award Amount: \$20,000  
Total Award Period Covered: 04/01/2015–09/30/2015  
Location of Project: Huntsville, Alabama  
Person-Months Per Year Committed to the Project. 3 months,

#### Pending

None, other than this.

### Dr. Bogdan Udrea

#### Current:

Total Award Period Covered: 1/1/2013-9/29/2015  
Principal Investigator: Bogdan Udrea  
Total Award Amount: \$110,000  
Project/Proposal Title: Arapaima - Low Cost CubeSat Mission for Three Dimensional Imaging  
Source of Support: US Air Force, Office of Scientific Research  
Principal Investigator: Bogdan Udrea  
Total Award Period Covered: 3/15/2015 3/14/2016  
Total Award Amount: \$3,000  
Project/Proposal Title: RASC-AL Competition Awards 2015  
Source of Support: National Institute of Aerospace

#### Pending:

Total Award Period Covered: 9/1/2015-8/31/2017